

GraFITi: Forecasting Irregularly Sampled Time Series using Graphs

Vijaya Krishna Yalavarthi,¹ Kiran Madusudanan,¹ Randolph Sholz¹ Nourhan Ahmed,¹ Johannes Burchert,¹ Shayan Javed¹ Stefan Born² Lars Schmidt-Thieme¹

¹ ISMLL, University of Hildesheim, Germany

{yalavarthi, kiranmadhusud, sholz, ahmedn, burchert, shayan, schmidt-thieme}@ismll.uni-hildesheim.de,

² Institute of Mathematics, TU Berlin, Germany

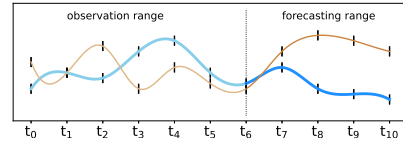
born@math.tu-berlin.de

Abstract

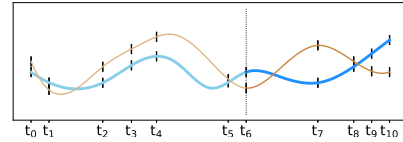
Forecasting irregularly sampled time series with missing values is a crucial task for numerous real-world applications such as healthcare, astronomy, and climate sciences. State-of-the-art approaches to this problem rely on Ordinary Differential Equations (ODEs), but are known to be slow and to require additional features to handle missing values. To address this issue, we propose a novel model using Graphs for Forecasting Irregularly Sampled Time Series with missing values which we call GraFITi. GraFITi first converts the time series to a Sparsity Structure Graph which is a sparse bipartite graph, and then reformulates the forecasting problem as the edge weight prediction task in the graph. It uses the power of Graph Neural Networks to learn the graph and predict the target edge weights. We show that GraFITi can be used not only for our Sparsity Structure Graph, but also for alternative graph representations of time series. GraFITi has been tested on 3 real-world and 1 synthetic irregularly sampled time series dataset with missing values and compared with various state-of-the-art models. The experimental results demonstrate that GraFITi improves the forecasting accuracy up to 17% and reduces the run time upto 5 times compared to the state-of-the-art forecasting models.

1 Introduction

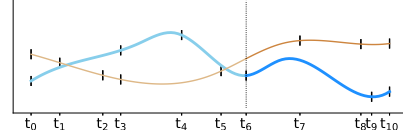
Time series forecasting is the task of predicting future values based on past observations. While it has been widely studied (Lim and Zohren 2021; Zeng et al. 2022; De Gooijer and Hyndman 2006) for past few decades, research in this domain is heavily focused on regularly sampled and fully observed multivariate time series (MTS). A little attention is given to irregularly sampled time series data with missing values (IMTS) which are often seen in many real-world applications. In IMTS, each channel is observed independently at irregular intervals which makes the time series extremely sparse when aligning it. The focus of this paper is forecasting of IMTS. Note that there is another variety of time series called irregular multivariate time series which is fully observed, but at irregular periods of time. We demonstrate the difference between forecasting of regular multivariate time series, irregular multivariate time series and irregularly sampled multivariate time series with missing values in Figure 1.



(a) Forecasting of regular multivariate time series



(b) Forecasting of irregular multivariate time series



(c) Forecasting of irregularly sampled multivariate time series with missing values

Figure 1: (a) multivariate time series forecasting, (b) irregular multivariate time series forecasting, (c) forecasting irregularly sampled multivariate time series with missing values. In all cases the observation range is from time t_0 to t_6 and the forecasting range is from time t_7 to t_{10} .

Ordinary Differential Equations (ODEs) are a well studied class of models for continuous time series, being used in many fields, including biology, physics and chemistry, to model the evolution of systems over time. Through modeling the rate of change of the state variables as a function of the state itself, as shown in Eq. 1, ODE-based models are able to predict at arbitrary time points in the future.

$$\frac{d}{dt}x(t) = f(t, x(t)) \quad (1)$$

Although ODE models can handle irregularity in the time series by continuous modeling of time, most of them (Chen et al. 2018; De Brouwer et al. 2019; Rubanova, Chen, and Duvenaud 2019; Biloš et al. 2021) cannot directly handle missing values in the observation

range of the time series. Hence, they rely on missing value indicators which is a series mask used as additional channels in the time series in order to handle sparsity. Usually both the observation values and missing values are seen as different scalar variables and the relation between them is not modeled explicitly. This adds an additional burden on the model to learn their relationship, with possible negative consequences for model performance. Another disadvantage of ODE models is, that they are often slow compared to non-ODE models, as shown in the literature for related tasks such as classification (Horn et al. 2020; Shukla and Marlin 2021) and interpolation (Shukla and Marlin 2021) of IMTS.

In this paper, we propose a novel model called GraFITi: graphs for forecasting irregularly sampled time series with missing values. In this approach, IMTS data is transformed into a Sparsity Structure Graph and forecasting is reformulated as the edge weight prediction in the graph. The channels and timepoints are represented as disjoint sets of nodes, connected by edges, which represent the observation values and the target values, hence avoiding the requirement of missing value indicators in the observed range. The forecasting problem is represented as the edge weight prediction in the graph. After converting a time series to its (sparsity structure) graph, GraFITi employs multiple graph neural network GNN layers consisting of attention (Vaswani et al. 2017) and feed forward layers to learn the interactions between nodes and edges. Finally, forecasts are provided as the edge weights of the last gnn layer. Our Sparsity Structure Graph, by design, provides a more dynamic and adaptive approach to process IMTS data, and improves the performance of the forecasting task.

Additionally, we describe two alternative graph representations of a time series. We demonstrate the versatile architecture of GraFITi by using it with different such graph representations for forecasting. We conducted a comprehensive study using 3 real-world and 1 synthetic dataset to evaluate the performance of GraFITi for forecasting IMTS. We compared GraFITi to various state-of-the-art forecasting methods designed for irregularly sampled time series as well as a selection of baselines that are geared towards regularly sampled time series. The results of our experiments demonstrate that GraFITi outperforms all the other models and provides superior forecasts.

Our contributions are summarized as follows:

- We propose a novel model called GraFITi for forecasting of IMTS. GraFITi represents the IMTS as a sparsity structure graph, which naturally avoids the missing values in the observation range of the time series (section 4).
- To the best of our knowledge, we are the first to represent IMTS as a Graph covering both time points and the channels as the nodes of the graph, unlike existing works where only channels are considered as graph nodes.
- GraFITi reframes IMTS forecasting as an instance of edge weight prediction in the graph (section 4) and uses the power of Graph Neural Networks in order to predict the weight of the target edge (section 6).
- Extensive experimental evaluation on 4 datasets that include 3 real world and 1 synthetic dataset shows that

GraFITi improves the forecasting accuracy of the best existing IMTS forecasting model upto 17% and the run time improvement up to 5 times (section 7).

In order to promote reproducibility, we provide the source code in <https://anonymous.4open.science/r/GraFITi-8F7B>.

2 Related Work

This work focus on the forecasting of irregularly sampled multivariate time series data with missing values using graphs. In this section, we discuss the research done in: forecasting of MTS, Graphs for MTS, forecasting models for IMTS, and graph neural network models .

Forecasting of MTS Forecasting multivariate time series (MTS) has traditionally been done using statistical methods such as auto-regressive models (Newbold 1983) and exponential time smoothing (Brocklebank and Dickey 2003) models. With the advent of machine learning and deep learning, a wide variety of new models have been proposed. These include models based on Convolutional Neural Networks (CNNs) (Oord et al. 2016; Borovykh, Bohte, and Oosterlee 2017), Recurrent Neural Networks (RNNs) (Sagheer and Kotb 2019; Siami-Namini, Tavakoli, and Namin 2019), and Transformer models (Zhou et al. 2021, 2022; Wu et al. 2021) (we study graphs for MTS later in a separate section) and the combinations (Livieris, Pintelas, and Pintelas 2020; Li et al. 2019). In recent years, Transformer-based models have shown to have superior performance compared to CNN and RNN based models. One such model, Informer, gained significant attention from the research community due to its novel sparse attention mechanism called “Probsparse Attention”. Currently, FedFormer is considered the state-of-the-art Transformer-based model for MTS forecasting. However, simple models such as DLinear and NLinear (Zeng et al. 2022), which only use linear layers, have demonstrated better performance. More detailed information on MTS forecasting models can be studied in recent survey paper (Lim and Zohren 2021). The major limitation of all these models is that they are developed only for MTS data and is challenging to adapt them to the IMTS setup.

Using graphs for MTS In addition to CNN, RNNs, and Transformers, graphs have been studied for the forecasting of IMTS. One of the early GNN-based approaches for multivariate time series forecasting is presented in (Wu et al. 2020), which requires a pre-defined adjacency matrix to define the relationships between the channels in the time series. However, more recent models such as Spectral Temporal Graph Neural Network (Cao et al. 2020) (STGNN) and Time-Aware Zigzag Network (Chen, Segovia, and Gel 2021) have sought to improve upon this approach by leveraging the properties of GNNs to capture the dependencies between the variables in a multivariate time series. These models connect all the nodes (channels of the multivariate time series) to learn the dependencies, which can be computationally expensive. In contrast, (Satorras, Rangapuram, and Januschowski 2022) proposed

a bipartite setup with induced nodes to reduce the complexity of the graph, which is built only using the channels. However, to the best of our knowledge, all existing time series forecasting models that use graph try to learn the correlation or similarity between the channels of the multivariate time series. They do not fully exploit the graph structure in the time series for forecasting. On the other hand, recently, Cini et.al., proposed Graph Neural Networks for the imputation of MTS. They treat MTS as sequence of graphs where edges represent the correlation among the edges. A recurrent neural network is used to process the sequence. Again, similar to above studies it works by learning similarity or correlation among the channels.

Forecasting of IMTS Research on irregularly sampled multivariate time series (IMTS) has mainly focused on classification (Li and Marlin 2015; Lipton, Kale, and Wetzel 2016; Rubanova, Chen, and Duvenaud 2019; Shukla and Marlin 2021; Tashiro et al. 2021; Horn et al. 2020; Tashiro et al. 2021) and interpolation (Che et al. 2018; Rubanova, Chen, and Duvenaud 2019; Shukla and Marlin 2021; Tashiro et al. 2021; Shukla and Marlin 2022; Yalavarthi, Burchert, and Schmidt-Thieme 2022b), with limited attention given to forecasting tasks. A majority of the models developed for these tasks are based on Neural Ordinary Differential Equations (ODEs)(Che et al. 2018). In(Rubanova, Chen, and Duvenaud 2019), an ODE was combined with a Recurrent Neural Network (RNN) to update the state at the point of new observation. Later, the GRU-ODE-Bayes model (De Brouwer et al. 2019) improved upon the standard ODE-RNN by incorporating the properties of Gated Recurrent Units (GRUs), ODEs, and Bayesian inference for the parameter estimation of the ODEs. Recently, the Latent Linear ODEs with Neural Kalman Filtering (LinODENet) model (Anonymous 2023) was proposed which uses a state-space model whose dynamics are governed by a linear ODE. It includes Kalman filtering, which helps to satisfy the self-consistency property, meaning the state of the model changes only if the observation differs from the model prediction. However, a significant limitation of all ODE-based models is that they are slow and typically require missing value indicators to handle missing values in IMTS, with the exception of LinODENet. In addition to ODEs, another branch of study uses Neural Flows (Biloš et al. 2021). These models (such as ResNET, GRU, and Coupling flows) learn a neural network to model the solution curves of ODEs, making the ODE integrator obsolete. Among different types of flows, GRU flows have been shown to perform well.

Graph Neural Networks Graph Neural Networks (GNNs) are developed to process the data that is represented as graphs. While most of literature in Graph Neural Networks such as Graph Convolutional Networks, Graph Attention Networks, deal with the problem of node classification (Kipf and Welling 2017; Velickovic et al. 2017), a few studied the task of the edge weight prediction. Bulk of literature (De Sá and Prudêncio 2011; Fu et al. 2018) in this domain performed the task relying on the latent features and graph heuristics such as node similarity (Zhao et al. 2015),

proximity (Murata and Moriyasu 2007) measures and local rankings (Yang and Wang 2020). Recently, deep learning based approaches (Hou and Holder 2017; Zulaika et al. 2022; You et al. 2020) were proposed. Other branch of the field studies the problem of edge weight prediction in the signed graph (Kumar et al. 2016), tailored to social networks, where the edge takes only the value between $[-1, 1]$. However, all the proposed methods perform edge weight prediction in a transductive setup where the entire data is a single graph and is split into training and testing which is not applicable to our case because our dataset consists of multiple graphs where a model needs to be trained on the train partition and evaluate it on the test set.

Delineating from GRAPE (You et al. 2020) Jiaxuan et al. introduced GRAPE, a graph-based model for imputing and classifying vector datasets with missing values. It uses a bipartite graph with sample IDs and variables as disjoint sets of nodes, and the edges representing the values of the variable in that sample. GRAPE trains the model in a transductive manner, with all data samples, including those from the test set, present in the graph. In contrast, GraFITi is designed for time series data, using a different graph structure where channels and time points are disjoint sets of nodes and time series observations are the edges connecting them, and it employs an inductive learning approach for the training process.

3 The Time Series Forecasting Problem

An **irregularly sampled multivariate times series with missing values**, is a finite sequence of pairs $S = (t_n, x_n)_{n=1:N}$ where $t_n \in \mathbb{R}$ is the n -th **observation time-point** and $x_n \in (\mathbb{R} \cup \{\text{NaN}\})^C$ is the n -th **observation event**. Components with $x_{n,c} \neq \text{NaN}$ represent **observed values** by channel c at event time t_n , and $x_{i,c} = \text{NaN}$ represents a missing value. C is the total number of channels.

A **time series query** is a pair (Q, S) of a time series S and a sequence $Q = (q_k, c_k)_{k=1:K}$ such that the value of channel $c_k \in \{1, \dots, C\}$ is to be predicted at time $q_k \in \mathbb{R}$. We call a query a **forecasting query**, if all its query timepoints are after the last timepoint of the time series S , an **imputation query** if all of them are before the last timepoint of S and a **mixed query** otherwise. In this paper, we are interested in forecasting only.

A vector $y \in \mathbb{R}^K$ we call an **answer** to the forecasting query: y_k is understood as the predicated value of time series S at time q_k in channel c_k . The difference between two answers y, y' to the same query can be measured by any loss function, for example by a simple squared error

$$\ell(y, y') := \frac{1}{K} \sum_{k=1}^K (y_k - y'_k)^2$$

The **time series forecasting problem** is as follows: given a dataset of pairs $D := (Q_i, S_i, y_i)_{i=1:M}$ of forecasting queries and ground truth answers from an unknown distribution p^{data} and a loss function ℓ on forecasting answers, find a forecasting model \hat{y} that maps queries (Q, S) to answers $\hat{y}(Q, S)$ such that the expected loss between ground

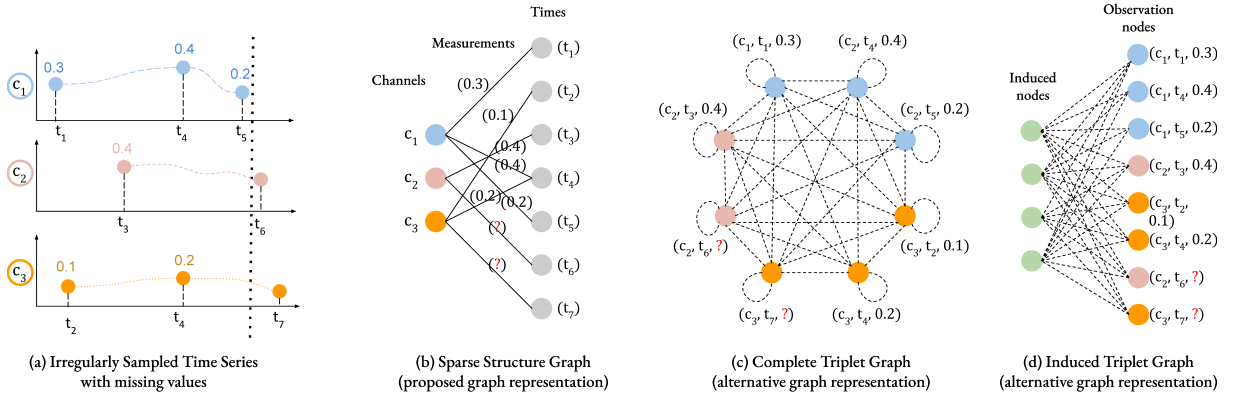


Figure 2: Representation of IMTS using graphs. (a) is an IMTS, (b) is the Full graph representation of (a) with all the observations as nodes and are densely connected which is similar to a Multi-head attention, (c) is the Induced graph representation where edges are connected according to the operations in a Induced multi-head attention, and (d) is our proposed sparse bipartite graph representation of IMTS where times and channels are the nodes and observation measurements as the edges.

truth answers and forecasted answers is minimal:

$$\mathcal{L}(\hat{y}; p^{\text{data}}) := \mathbb{E}_{(Q, S, y) \sim p^{\text{data}}} [\ell(y, \hat{y}(Q, S))]$$

4 Sparsity Structure Graph Representation

We describe the proposed Sparsity Structure Graph representation and convert the forecasting problem as edge weight prediction problem. The motivation behing this is:

- We explicitly obtain the relationship between the channels and observation times via measurement values allowing the inductive bias of the data to pass into the model.
- We avoid learning the MVIs. While ODEs work on MVIs, research in adjacent tasks such as Classification (Shukla and Marlin 2021; Horn et al. 2020; Yalavarthi, Burchert, and Schmidt-Thieme 2022a) and Interpolation of IMTS (Shukla and Marlin 2021, 2022; Yalavarthi, Burchert, and Schmidt-Thieme 2022b) shows that the models without MVI in observation space perform better than the ones with.

Missing values represented by NaN-values are unsuited for standard arithmetical operations. Therefore, they are often encoded by dedicated binary variables called **missing value indicators** or masks: $x_n \in (\mathbb{R} \times \{0, 1\})^C$. Here, $(x_{n,c}, 1)$ encodes an observed value and $(0, 0)$ encodes a missing value. Usually, both components are seen as different scalar variables: the real value and its binary missing value indicator / mask, the relation between both is dropped and observations simply modeled as $x_n \in \mathbb{R}^{2C}$.

For time series classification and imputation problems, dedicated sparse representations of time series have been developed: **the triplet representation** (Horn et al. 2020) represents a sparse time series $S = (t_n, x_n)_{n=1:N}$ as a set of observation triples

$$\begin{aligned} \text{ts2triplets}(S) &:= \{(t_n, c, x_{n,c}) \mid x_{n,c} \neq \text{NaN}\} \\ &:= \{(\tilde{t}_j, c_j, o_j) \mid j = 1 \dots N_s\} \end{aligned}$$

where $N_s := |\{(n, c) \mid x_{n,c} \neq \text{NaN}\}|$ is the total number of observations across all channels, while o_j is the observation value made by $c_j \in \{1, \dots, C\}$ at time $\tilde{t}_j \in \{t_1, \dots, t_N\}$.

We propose a novel representation of a time series S as a bipartite graph $G = (V, E)$ with nodes $V = V_C \dot{\cup} V_T$ for channels and timepoints and edges E between each channel and timepoint node with an observation, having the value as edge features F_{edge} and the channel IDs and timepoints as node features F_{node} . Nodes $V_C := \{1, \dots, C\}$ represent channels and nodes $V_T := \{C + 1, \dots, C + N\}$ represent unique timepoints:

$$\begin{aligned} V &:= \{1, \dots, C + N\} = V_C \dot{\cup} V_T \\ E &:= \{\{i, j\} \mid x_{i-C,j} \neq \text{NaN}, i \in V_T, j \in V_C\} \\ F_v^{\text{node}} &:= \begin{cases} v &: v \in V_C \\ t_j &: v \in V_T, j = v - C \end{cases} \\ F_e^{\text{edge}} &:= x_{i-C,j} \quad \text{for } e = \{i, j\} \in E \quad \text{with } i \in V_T, j \in V_C \end{aligned} \quad (2)$$

For an IMTS, missing values make the bipartite graph sparse meaning $|E| \ll C \cdot N$. However, for a fully observed time series, where there are no missing values, i.e. $|E| = C \cdot N$, the graph is a complete bipartite graph.

We extend this representation to time series queries (S, Q) by adding additional edges between queried channels and timepoints and distinguish observed and queried edges by an additional binary edge feature. Note that the target indicator used to differentiate the observed edge and target edge is different from the missing value indicator which is used to represent the missing observations in the observation space. Given a query $Q = (q_k, c_k)_{k=1:K}$, let $(t'_1, \dots, t'_{K'})$ be an enumeration of the unique queried timepoints q_k . We introduce additional nodes $V_Q := \{C + N + 1, \dots, C + N + K'\}$ so that the augmented graph, together with the node and

edge features is given as

$$\begin{aligned}
V &:= V_C \dot{\cup} V_T \dot{\cup} V_Q = \{1, \dots, C + N + K'\} \\
E &:= \{(i, j) \mid x_{i-C, j} \neq \text{NaN}, i \in V_T, j \in V_C\} \\
&\cup \{(i, j) \mid i \in V_Q, j \in V_C, (t'_{i-N-C}, j) \in Q\} \\
F_v^{\text{node}} &:= \begin{cases} v : v \in V_C \\ t_j : v \in V_T, j = v - C \\ t'_j : v \in V_Q, j = v - C - N \end{cases} \\
F_e^{\text{edge}} &:= \begin{cases} (x_{i,j}, 1) : e = \{i, j\} \in E \text{ with } i \in V_T, j \in V_C \\ (0, 0) : e = \{i, j\} \in E \text{ with } i \in V_Q, j \in V_C \end{cases} \quad (3)
\end{aligned}$$

where $(t'_{i-N-C}, j) \in Q$ is supposed to mean that (t'_{i-N-C}, j) appears in the sequence Q . To denote this graph representation, we write briefly

$$\text{ts2graph}(X, Q) := (V, E, F^{\text{node}}, F^{\text{edge}}) \quad (4)$$

To make the graph representation $(V, E, F^{\text{node}}, F^{\text{edge}})$ of a time series query processable by a graph neural network, node and edge features have to be properly embedded, otherwise, both, the nominal channel ID and the timepoint are hard to compute on. We propose an **Initial Embedding layer** that encodes channel IDs via a onehot encoding and time points via a learned sinusoidal encoding (Shukla and Marlin 2021):

$$h_v^{\text{node},0} := \begin{cases} \mathbf{FF}(\text{onehot}(F_v^{\text{node}})) : v \in V_C \\ \sin(\mathbf{FF}(F_v^{\text{node}})) : v \in V_T \dot{\cup} V_Q \end{cases} \quad (5)$$

$$h_e^{\text{edge},0} := \mathbf{FF}(F_e^{\text{edge}}) \text{ for } e \in E \quad (6)$$

where onehot denotes the binary indicator vector and \mathbf{FF} denotes a separate fully connected layer in each case.

The final graph neural network layer $(h^{\text{node},L}, h^{\text{edge},L})$ has embedding dimension 1. The scalar values of the query edges are taken as the predicted answers to the encoded forecasting query:

$$\hat{y} := \text{graph2ts}(h^{\text{node},L}, h^{\text{edge},L}) = (h_{e_k}^{\text{edge},L})_{k=1:K} \quad (7)$$

$$\text{where } e_k = \{C + N + k', c_k\} \text{ with } t'_k = q_k$$

5 Alternative Graph Representations of Time Series

The Sparsity Structure Graph is a novel representation of IMTS proposed in this work. However, other representations exist, including the Complete Triplet graph which is based on the triplet representation, and the Induced Triplet graph which utilizes induced attention to simplify the Complete Triplet graph.

5.1 Complete Triplet Graph Representation.

The triplet representation $(\tilde{t}_j, c_j, o_j)_{j=1:N_s}$ also could be interpreted as a simpler, alternative graph representation of a time series. Nodes are triples, all nodes are connected, so we have a complete graph, node features are the triplets and there are no edge features:

$$\begin{aligned}
V &:= V_{T_s} = \{1, \dots, N_s\} & F_v^{\text{node}} &:= (\tilde{t}_v, c_v, o_v) \\
E &:= \{(i, j) \mid i, j \in V\} & F^{\text{edge}} &:= \emptyset
\end{aligned} \quad (8)$$

Also this representation can be extended to time series queries $(S, Q) = ((t_n, x_n)_{n=1:N}, (q_k, c_k)_{k=1:K})$ in a respective manner:

$$\begin{aligned}
V &:= V_{T_s} \dot{\cup} V_Q = \{1, \dots, N_s + K\} \\
E &:= \{(i, j) \mid i \neq j\} \\
F_v^{\text{node}} &:= \begin{cases} (\tilde{t}_v, c_v, o_v, 1) : v \in V_{T_s} \\ (q_k, c_k, 0, 0) : v \in V_Q, k = v - N_s \end{cases} \\
F^{\text{edge}} &:= \emptyset
\end{aligned} \quad (9)$$

The 4th node feature now is the binary predictor indicator, which is 1 for observed values and 0 for target values. Node features again have to be encoded in a suitable manner respecting the feature types:

$$h_v^{\text{node},0} := \sin(\mathbf{FF}(F_{v,1}^{\text{node}})) + \mathbf{FF}(\text{onehot}(F_{v,2}^{\text{node}})) + \mathbf{FF}(F_{v,3:4}^{\text{node}})$$

where again \mathbf{FF} denotes independent feedforward layers.

The final node features are used as prediction:

$$\hat{y} := (h_{N_s+k}^{\text{node},L})_{k=1:K}$$

5.2 Induced Triplet Graph Representation.

While the complete triplet graph representation allows representing dependencies between any two observations across different times and channels, it also suffers from a quadratic complexity $\mathcal{O}((N_s + K)^2)$ in the number of triplets / non-zeros and the queries. To counteract this problem, one can adapt an idea from the SetTransformer (Lee et al. 2019), that models the relation not between pairs of elements in a set, but uses a bipartite structure between elements and artificial hidden nodes, called induced nodes, thus modeling relations between elements only indirectly via the induced nodes and breaking the quadratic complexity to $\mathcal{O}(M(N_s + K))$ by doing so. With M induced nodes $V_M := \{1, \dots, M\}$:

$$\begin{aligned}
V &:= V_M \dot{\cup} V_{T_s} = \{1, \dots, M + N_s\} \\
E &:= \{(i, j) \mid i \in V_{T_s}, j \in V_M\} \\
F_v^{\text{node}} &:= \begin{cases} v : v \in V_M \\ (\tilde{t}_j, c_j, o_j) : v \in V_{T_s}, j = v - M \end{cases} \\
F^{\text{edge}} &:= \emptyset
\end{aligned} \quad (10)$$

Extended to queries:

$$\begin{aligned}
V &:= V_M \dot{\cup} V_{T_s} \dot{\cup} V_Q = \{1, \dots, M + N_s + K\} \\
E &:= \{(i, j) \mid i \in V_{T_s} \dot{\cup} V_Q, j \in V_M\} \\
F_v^{\text{node}} &:= \begin{cases} v : v \in V_M \\ (\tilde{t}_j, c_j, o_j, 1) : v \in V_{T_s}, j = v - M \\ (q_k, c_k, 0, 0) : v \in V_Q, k = v - M - N_s \end{cases} \\
F^{\text{edge}} &:= \emptyset
\end{aligned} \quad (11)$$

Suitable encoding and decoding layers for this graph:

$$\begin{aligned}
h_v^{\text{node},0} &:= \begin{cases} \mathbf{FF}(\text{onehot}(F_v^{\text{node}})) & : v \in V_M \\ \sin(\mathbf{FF}(F_{v,1}^{\text{node}})) + \mathbf{FF}(\text{onehot}(F_{v,2}^{\text{node}})) & : \text{else} \\ + \mathbf{FF}(F_{v,3:4}^{\text{node}}) \end{cases} \\
\hat{y} &:= (h_{M+N_s+k}^{\text{node},L})_{k=1:K}
\end{aligned}$$

Delineation from the Sparsity Structure Graph. Induced nodes V_M in the Induced Triplet Graph are similar to the channel nodes V_C in the Sparsity Structure Graph. However, in the Sparsity Structure Graph representation, channels are connected to timepoints V_T in the graph and have additional information, while the induced nodes in the Induced Triplet Graph only exist to provide additional connections to V_{Ts} and do not have any information regarding the series. Hence, by design the Sparse Structure Graph allows the inductive bias of the time series to flow into the (GraFITi) model, that we discuss in next Section, by exploiting the time channel relationships which is not the case with Induced Triplet Graph (and Complete Triplet Graph).

6 Forecasting with GraFITi

GraFITi can process all the three representations: Sparsity Structure Graph, Complete Triplet Graph, and Induced Triplet Graph. In this Section, first, we explain the functioning of GraFITi for the proposed Sparsity Structure Graph and discuss the extension to the alternative graph representations at the end.

GraFITi first encodes the time series query to graph using Eq. 4 and compute initial embeddings for the nodes ($h_{node,0}$) and edges ($h_{edge,0}$) using Eqs. 5 and 6 respectively. Now, we can leverage the power of graph neural networks for further processing the encoded graph. Node and edge features are updated layer wise, from layer l to $l+1$ using a graph neural network (GNN):

$$(h^{\text{node},l+1}, h^{\text{edge},l+1}) := \text{gnn}^{(l)}(h^{\text{node},l}, h^{\text{edge},l}, V, E)$$

There have been variety of gnn architectures as such as Graph Convolutional Networks (Kipf and Welling 2017), Graph Attention Networks (Velickovic et al. 2017), exist in the literature. In this work, we propose a model adapting the Graph Attention Network (Velickovic et al. 2017) to our graph setting and incorporate various important components to cater for sparsity structure graph setup. While the attention weights in the Graph Attention (Velickovic et al. 2017) are computed by adding queries and keys, the standard attention uses multiplication of queries and keys. We verified both the attention models and did not find any advantage of Graph attention; and hence we use standard attention mechanism, in our attention block (we discuss soon), as it has been widely used in the literature (Zhou et al. 2021). Additionally, We also use edge embeddings in our setup to update node embedding in a principled manner.

Graph Neural Network (gnn)

First, we define Multi-head Attention block (**MAB**) and Neighborhood functions that are used in our gnn .

Multi-head attention block (**MAB**) (Vaswani et al. 2017) is represented as:

$$\mathbf{MAB}(\mathcal{Q}, \mathcal{K}, \mathcal{V}) := \alpha(\mathcal{H} + \mathbf{FF}(\mathcal{H}))$$

where $\mathcal{H} := \alpha(\mathcal{Q} + \mathbf{MHA}(\mathcal{Q}, \mathcal{K}, \mathcal{V}))$

where \mathcal{Q}, \mathcal{K} and, \mathcal{V} are called queries, keys, and values respectively, **MHA** is multi-head attention (Vaswani et al. 2017), α is a non-linear activation.

Algorithm 1 Graph Neural Network

Require: $h^{\text{node}, t}, h^{\text{edge}, t}, V, E$

```

1: for  $u \in V$  do
2:    $H_u \leftarrow ([h_v^{\text{node},l} \parallel h_e^{\text{edge},l}])_{v \in \mathcal{N}(u)}$  // $e = \{u, v\}$ 
3:    $h_u^{\text{node},l+1} \leftarrow \mathbf{MAB}^{(l)}(h_u^{\text{node},l}, H_u, H_u)$ 
4: end for
5: for  $e = \{u, v\} \in E$  do
6:    $h_e^{\text{edge},l+1} \leftarrow \alpha \left( h_e^{\text{edge},l} + \mathbf{FF}^{(l)} \left( [h_u^{\text{node},l} \parallel h_v^{\text{node},l} \parallel h_e^{\text{edge},l}] \right) \right)$ 
7: end for
8: return  $h^{\text{node},l+1}, h^{\text{edge},l+1}$ 

```

Neighborhood of a node u is defined as the set of all the nodes connected to u through edges in E which can be given as follows:

$$\mathcal{N}(u) \coloneqq \{v \mid \{u, v\} \in E\} \quad (12)$$

GraFITi consists of L many gnn layers. In the layer l , each node $u \in V$ is updated using the embeddings of its neighborhood nodes $h_v^{\text{node},l}, v \in \mathcal{N}(u)$, and edges $h_e^{\text{edge},l}, e = \{u, v\} \in E$ connecting them by employing **MAB**. On the other hand, for an edge $e = \{u, v\} \in E$, we compute edge embedding $h_e^{\text{edge},l+1}$ using the embedding of the nodes connected to it $h_u^{\text{node},l}, h_v^{\text{node},l}$, and its own previous embedding vector $h_e^{\text{edge},l}$. After passing the graph to L many layers of gnn we predict the answers to the queries. Overall architecture of GraFITi algorithm is presented in Figure 3.

Update node embeddings In order to update embedding of a node $u \in V$, first, we create a sequence of features H_u where each feature is a concatenation of the node embedding $h_v^{\text{node},l}$ and edge embedding $h_e^{\text{edge},l}$, $e = \{u, v\}$ where $v \in \mathcal{N}(u)$. Then, we pass $h_u^{\text{node},l}$ as queries and H_u as keys and values to MAB.

$$h_u^{\text{node},l+1} := \mathbf{MAB}^{(l)} \left(h_u^{\text{node},l}, H_u, H_u \right) \quad (13)$$

$$H_u := ([h_v^{\text{node},l} \parallel h_e^{\text{edge},l}])_{v \in \mathcal{N}(u)}, \quad e = \{u, v\} \quad (14)$$

Updating edge embeddings: In order to compute $h_e^{\text{edge},l+1}$, $e = \{u, v\}$ we concatenate $h_u^{\text{node},l}, h_v^{\text{node},l}$ and $h_e^{\text{edge},l}$, and pass it through a dense layer (FF) followed by a residual connection and nonlinear activation.

$$h_e^{\text{edge},l+1} := \alpha \left(h_e^{\text{edge},l} + \mathbf{FF}^{(l)} \left(h_u^{\text{node},l} \parallel h_v^{\text{node},l} \parallel h_e^{\text{edge},l} \right) \right) \quad (15)$$

where $e = \{u, v\}$. Note that, although our edges are undirected, we compute the edge embedding by concatenating the embeddings in a specific order i.e., the channel embedding, time embedding and edge embedding. We show the process of updating nodes and edges in layer l using a gnn in Algorithm 1.

Answering the queries: As mentioned Section 4, our last gnn^(L) layer have the embedding dimension of 1. Hence, after processing the graph features through L many gnn layers, we use Eq. 7 to decode the graph and provide the predicted answers to the time series query. Forward pass of GraFITi is presented in Algorithm 2.

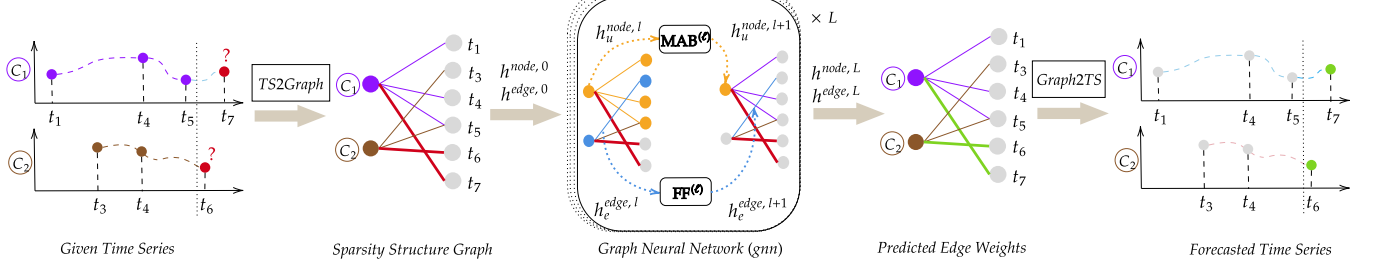


Figure 3: Overall architecture of GraFITi.

Algorithm 2 Forward pass of GraFITi

```

Require: Observed time series forecasting query  $(S, Q)$ 
1:  $(V, E, F_{\text{node}}, F_{\text{edge}}) \leftarrow \text{ts2graph}(S, Q)$ 
   //Initial embeddings of nodes and edges
2:  $h_{\text{node},0} \leftarrow \{h_{u,0} \mid u \in V\}$                                 //using Eq. 5
3:  $h_{\text{edge},0} \leftarrow \{h_{u,v,0} \mid \{u, v\} \in E\}$                       //using Eq. 6
   //Graph Neural Network
4: for  $l \in \{1, \dots, L\}$  do
5:    $h_{\text{node},l+1}, h_{\text{edge},l+1} \leftarrow \text{gnn}^{(l)}(h_{\text{node},l}, h_{\text{edge},l}, V, E)$ 
6: end for
7:  $\hat{y} \leftarrow \text{graph2ts}(h_{\text{node},L}, h_{\text{edge},L}, V)$ 
8: return  $\hat{y}$ 

```

Computational Complexity: The computational complexity of the GraFITi lies mostly in the usage of **MAB** in Eq. 13. The complexity of computing the embedding of a single channel node $u \in \{1, \dots, C\}$ is at maximum $\mathcal{N}(u)$ because only neighborhood connections are used for updating the channel node embedding and $\mathcal{N}(u) \subseteq \{C+1, \dots, C+N+K'\}$. Hence computing the embedding of all the channel nodes will be $\mathcal{O}(\sum_{u=1}^C \mathcal{N}(u))$ which is $\mathcal{O}(N_s)$. Similarly computational complexity of **MAB** in computing embedding of all the nodes in $V_T \cup V_Q$ is $\mathcal{O}(\sum_{u=1}^{N+K'} \mathcal{N}(u))$ which is again $\mathcal{O}(N_s)$. A feed forward layer **FF** : $\mathbb{R}^Y \rightarrow \mathbb{R}^Z$ will have a computational complexity of $\mathcal{O}(YZ)$.

GraFITi for alternate graph representations:

GraFITi can process the alternate graph representations mentioned in Section 5. Similar to above, GraFITi first converts the time series into alternate graph representations, and then create the initial embedding for nodes ($h_{\text{node},0}$) and edges ($h_{\text{edge},0}$) using the respective Initial Embedding layer. Then, the node and edge embedding are passed through L many gnn layers consisting of **MAB**. Here, because edges do not have any features, $h_{\text{edge},L} = \emptyset$. Again, the embedding of nodes in the last layer are 1 dimensional. Finally, the scalar values of the query nodes are taken as the predicted answers to the encoded forecasting query.

7 Experiments

We begin with the datasets used for the model evaluation.

Table 1: Statistics of the datasets used in the experiments. Sparsity means the percentage of missing observations in the time series

Name	#Sample	#Chann.	Max.len.	Max.Obs.	Sparsity
USHCN	1,100	5	290	320	77.9%
MIMIC-III	21,000	96	96	710	94.2%
MIMIC-IV	18,000	102	710	1340	97.8%
Physionet'12	12,000	37	48	520	85.7%

7.1 Dataset description

Four datasets including 3 real world and 1 synthetic IMTS are used for evaluating the proposed model. Basic statistics of the datasets is provided in Table 1.

Physionet2012 (Silva et al. 2012) is the collection of the records of 12,000 patients admitted to the ICU where over 37 vitals were measured for the first 48 hours of the admission. We follow the protocol used in previous studies (Che et al. 2018; Cao et al. 2018; Tashiro et al. 2021) and processed the dataset to hourly observations making a total of upto 48 observations in each series.

MIMIC-III (Johnson et al. 2016) is also a medical dataset consisting of the measurements of the ICU patients admitted at Beth Israel Hospital. Around 96 variables of 18,000 patients were observed for around 48 hours. We follow the preprocessing steps provided in in (Anonymous 2023; Biloš et al. 2021; De Brouwer et al. 2019) and rounded the observations into 30 minute intervals.

MIMIC-IV (Johnson et al. 2021) is built upon the MIMIC-III database and contains data of around 18,000 patients admitted to ICU at tertiary academic medical center in Boston where 102 many variables are monitored. We performed preprocessing of the dataset as given in (Anonymous 2023; Biloš et al. 2021) and rounded the observations to a minute interval.

USHCN (Menne, Williams Jr, and Vose 2015) is a climate dataset consists of the measurements of 5 variables (daily temperatures, precipitation and snow) observed over 150 years from 1218 meteorological stations in the USA. We followed the same pre-processing steps given in (Anonymous 2023; Biloš et al. 2021; De Brouwer et al. 2019) and selected a subset of 1114 stations and an observation window of 4 years (1996-2000).

7.2 Competing algorithms

Here, we provide the brief details of the models that are compared with the proposed GraFITi with Sparsity Structure Graph for the evaluation.

IMTS forecasting models *mTAN* (*Shukla and Marlin 2021*) is an interpolation model which can be adapted to the forecasting task. It encodes the IMTS to MTS using an attention layer and decodes the MTS to provide forecasts at target time points.

GRU-ODE-Bayes (*De Brouwer et al. 2019*) model is continuous-time version of GRU built upon the Neural ODEs (*Chen et al. 2018*) which uses a Bayesian update network for processing the observations in IMTS.

Neural Flows (*Biloš et al. 2021*) is a flow model that learn a neural network to model the solution curves of ODE making the ODE integrator obsolete. We use GRU as the flow architecture which showed promising results in (*Biloš et al. 2021*).

Latent Linear ODE (*Anonymous 2023*) is a state space model where latent space dynamics are governed by a Linear Neural ODE.

Additionally, we also compare with the published results from (*De Brouwer et al. 2019*) for the NeuralODE-VAE (*Chen et al. 2018*), NeuralODE-VAE-Mask (*Chen et al. 2018*), Sequential VAE (*Krishnan, Shalit, and Sontag 2015, 2017*), GRU-Simple (*Che et al. 2018*), GRU-D (*Che et al. 2018*) and T-LSTM (*Baytas et al. 2017*).

MTS forecasting models Bulk of literature studied the time series forecasting in MTS. Hence, it is interesting to see how the state-of-the-art MTS forecasting models perform in the IMTS setup. MTS forecasting models cannot process the IMTS directly. Hence, we add missing value indicators as the separate channels to the series and process the time series along with the missing value indicators. We compared with the following MTS forecasting models:

Informer+ is a variant of Informer (*Zhou et al. 2021*) one of the widely used MTS forecasting model. It uses Prob-sparse attention which reduces the computational complexity of canonical attention.

Fedformer+ is a variant of Fedformer (*Zhou et al. 2022*), the current state-of-the-art transformer based model for forecasting of MTS which has a novel architecture combining the Transformer with season-trend decomposition.

DLinear+ and *NLinear+* (*Zeng et al. 2022*) are the variants of the state-of-the-art MTS forecasting models DLinear and NLinear respectively, adapted to IMTS setup. They use simple linear layers for the forecasting. In DLinear, linear layers are applied on the decomposed time series (seasonality and trend) while NLinear implement linear layers directly.

7.3 Experimental setup

Task protocol We followed the same protocol used for the baseline models in (*Anonymous 2023; Biloš et al. 2021; De Brouwer et al. 2019*). We used 5-fold cross validation and the hyperparameters are selected using the holdout validation set (20%) and used 10% left-out unseen data for the

evaluation. We train all the models on the Mean Squared Error and use the same as the evaluation metric.

Hyperparameter search We searched the following hyperparameters for all GraFITi: #iterations $L \in \{1, 2, 3, 4\}$, #heads in **MAB** from $\{1, 2, 4\}$, and hidden nodes in dense layers from $\{16, 32, 64, 128, 256\}$. We followed the procedure set by (*Horn et al. 2020*) for selecting the hyperparameters. Specifically, we randomly sampled sets of different hyperparameters and choose the one that has the best performance on validation dataset for evaluation. We used Adam optimizer with learning rate of 0.001, and reduced the learning rate to half when validation loss did not improve for 10 epochs. We train all the models upto 200 epochs; use early stopping over validation loss and set the patience to 30 epochs. Hyperparameters searched for the based models are presented in the supplementary material.

All the models were experimented using the PyTorch library on a GeForce RTX-3090 GPU. To ensure reproducibility, we have made the source code of the model available at the following URL: <https://anonymous.4open.science/r/GraFITi-8F7B>. Mainly, we used the TSDM package provided in (*Anonymous 2023*) in order to run the experiments.

7.4 Experimental results

First, we set the observation and prediction range of the IMTS as mentioned in the previous works (*Anonymous 2023; Biloš et al. 2021; De Brouwer et al. 2019*). For the USHCN dataset, the model observes for the first 3 years and forecasts the next 3 time steps. For the medical datasets, the model observes for the first 36 hours in the series and predicts the next 3 time steps. The results, including the mean and standard deviation, are presented in Table 2. The best result is highlighted in bold and the next best in italics. Additionally, we also provide the published results from (*Anonymous 2023; Biloš et al. 2021; De Brouwer et al. 2019*) in brackets for comparison.

The proposed GraFITi model is shown to be superior compared to all baseline models across all the datasets. Specifically, in the MIMIC-III and MIMIC-IV datasets, GraFITi provides around 11.2% and 17.2% improvement in forecasting accuracy compared to the next best IMTS forecasting model LinODEnet. The results on the USHCN dataset have high variance, therefore, it is challenging to compare the models on this dataset. However, we followed the protocol of (*Anonymous 2023; De Brouwer et al. 2019*), and experimented on it for completeness. Again, we achieve the best result with 9.2% improvement compared to the next best model. We note that, the MTS forecasting models that are adapted for the IMTS task, perform worse than any of the IMTS forecasting models demonstrating the limitation of MTS models in applying for IMTS tasks.

Efficiency comparison Here, the efficiency of well-performing models for irregularly sampled time series forecasting is compared for all four datasets. The models being compared are GraFITi, LinODEnet, Neural Flow, and GRU-ODE-Bayes, in terms of both evaluation time (with batch

Table 2: Experimental results for forecasting next three time steps. Evaluation metric MSE, Lower is better. Best results are in bold and the next best are in *italics*. Published results are presented in open brackets, Physionet’12 dataset was not used by the baseline models hence do not have published results. We show % improvement with \uparrow . ‘ME’ indicates Memory Error.

	USHCN	MIMIC-III	MIMIC-IV	Physionet’12
DLinear+	0.347 ± 0.065	0.691 ± 0.016	0.577 ± 0.001	0.380 ± 0.001
NLinear+	0.452 ± 0.101	0.726 ± 0.019	0.620 ± 0.002	0.382 ± 0.001
Informer+	0.320 ± 0.047	0.512 ± 0.064	0.420 ± 0.007	0.347 ± 0.001
FedFormer+	2.990 ± 0.476	1.100 ± 0.059	2.135 ± 0.304	0.455 ± 0.004
NeuralODE-VAE	—	(0.960 ± 0.110)	—	—
NeuralODE-VAE-Mask	—	(0.830 ± 0.100)	—	—
Sequential VAE	—	(0.830 ± 0.070)	—	—
GRU-Simple	—	(0.750 ± 0.120)	—	—
GRU-D	—	(0.530 ± 0.060)	—	—
T-LSTM	—	(0.590 ± 0.110)	—	—
mTAN	0.300 ± 0.038	0.540 ± 0.036	ME	0.315 ± 0.002
GRU-ODE-Bayes	0.401 ± 0.089 (0.430 ± 0.070)	0.476 ± 0.043 (0.480 ± 0.010)	0.360 ± 0.001 (0.379 ± 0.005)	0.329 ± 0.004
Neural Flow	0.414 ± 0.102	0.477 ± 0.041 (0.490 ± 0.004)	0.354 ± 0.001 (0.364 ± 0.008)	0.326 ± 0.004
LinODEnet	0.300 ± 0.060 (0.290 ± 0.060)	0.446 ± 0.033 (0.450 ± 0.020)	0.272 ± 0.002 (0.274 ± 0.002)	0.299 ± 0.001
GraFITi (ours)	0.272 ± 0.047 $\uparrow 9.3\%$	0.396 ± 0.030 $\uparrow 11.2\%$	0.225 ± 0.001 $\uparrow 17.2\%$	0.286 ± 0.001 $\uparrow 4.3\%$

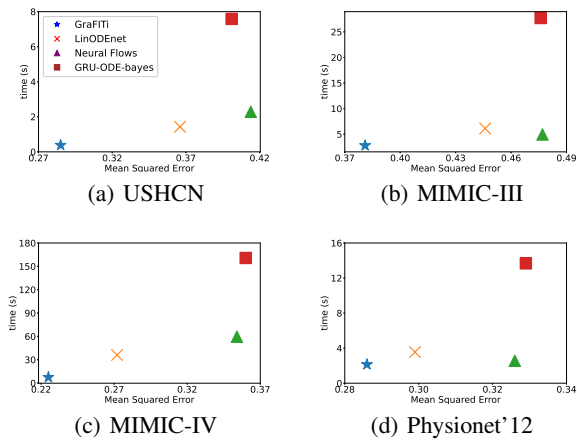


Figure 4: Comparison of IMTS forecasting models: GraFITi, LinODEnet, Neural Flows and GRU-ODE-Bayes in terms of efficiency: evaluation time against error metric.

size of 64) and error metric. The results are presented in Figure 4. The results demonstrate that for datasets with longer time series, such as the MIMIC-IV and USHCN dataset, the GraFITi is significantly faster than the ODE and flow-based models. Specifically, GraFITi is more than 5 times faster than the fastest ODE model, LinODEnet for both MIMIC-IV and USHCN. For datasets with shorter time series, such as Physionet’12 and MIMIC-III, GraFITi is still twice faster than LinODEnet. Additionally, GraFITi is faster than GRU-ODE-bayes by an order of magnitude on average.

Varying observation and forecast ranges This experiment is conducted with two different observation ranges (24 and 36 hours) and two different prediction ranges for each observation range. Specifically, for the observation range of 24 hours, the prediction ranges are 12 and 24 hours, and for the observation range of 36 hours, the prediction ranges are 6

and 12 hours. This approach allows for a more comprehensive evaluation of the model’s performance across various scenarios of observation and prediction ranges. The results are presented in Table 3.

We notice that the pattern seen with forecasting range of 3 time steps continues. GraFITi is the best performing model. The next best performing model is LinODEnet. We observe huge gains in forecasting accuracy for MIMIC-III and MIMIC-IV datasets. On an average GraFITi improved the forecasting accuracy of the LinODEnet (existing state-of-the-art IMTS forecasting model) by 8.5% in MIMIC-III, 15.5% in MIMIC-IV and 2.6% in Physionet’12 dataset.

7.5 GraFITi for alternative representations

Here, GraFITi is applied on top of alternative graph variants: Complete Triplet Graph and Induced Triplet Graph which are discussed in Section 5. Table 4 consists of the results for the real IMTS datasets with the observation range of 36 hours and the forecast range of 3 time points. GraFITi+SSG is same as GraFITi that uses Sparse Structure Graph, GraFITi+CTG is GraFITi for Complete Triplet Graph, and GraFITi+ITG is GraFITi for Induced Triplet Graph. GraFITi+SSG performs better than GraFITi+CTG and GraFITi+ITG on MIMIC-III and MIMIC-IV datasets, where as similar to GraFITi+CTP in Physionet’12 dataset. An interesting observation is that GraFITi+ITG, perform worse than GraFITi+SSG and GraFITi+CTG in all the datasets. The reason could be that the Induced attention, a key learning mechanism behind Induced graph, is proposed for encoder-decoder based architectures (Lee et al. 2019; Yalavarthi, Burchert, and Schmidt-Thieme 2022b). In these architectures, induced attention is applied on the encoder and **MAB** for the decoder. When induced mechanism is the only methodology for learning, it is providing poor performance (Yalavarthi, Burchert, and Schmidt-Thieme 2022b). This suggests that Induced attention may be more effective when used in conjunction with other attention mechanisms, such as **MAB**, in an encoder-decoder architecture. This bet-

Table 3: Experimental results on varying observation and forecasting ranges for the medical datasets. Evaluation measure is MSE. Lower is better. Best results are in bold and the second best are in italics.

	Obs. / Pred.	GraFITi (ours)	LinODEnet	Neural Flow	GRU-ODE-Bayes	\uparrow %
MIMIC-III	24/12	0.438 \pm 0.009	<i>0.477 \pm 0.021</i>	0.588 \pm 0.014	0.591 \pm 0.018	\uparrow 8.2%
	24/24	0.491 \pm 0.014	<i>0.531 \pm 0.022</i>	0.651 \pm 0.017	0.653 \pm 0.023	\uparrow 7.5%
	36/6	0.457 \pm 0.050	<i>0.492 \pm 0.019</i>	0.573 \pm 0.043	0.580 \pm 0.049	\uparrow 7.1%
	36/12	0.490 \pm 0.027	<i>0.554 \pm 0.042</i>	0.62 \pm 0.035	0.632 \pm 0.044	\uparrow 10.8%
MIMIC-IV	24/12	0.285 \pm 0.001	<i>0.335 \pm 0.002</i>	0.465 \pm 0.003	0.366 \pm 0.154	\uparrow 14.9%
	24/24	0.285 \pm 0.002	<i>0.336 \pm 0.002</i>	0.465 \pm 0.003	0.439 \pm 0.003	\uparrow 15.1%
	36/6	0.260 \pm 0.002	<i>0.309 \pm 0.002</i>	0.405 \pm 0.001	0.393 \pm 0.002	\uparrow 15.9%
	36/12	0.261 \pm 0.005	<i>0.309 \pm 0.002</i>	0.395 \pm 0.001	0.393 \pm 0.002	\uparrow 15.5%
Physionet'12	24/12	0.365 \pm 0.001	<i>0.373 \pm 0.001</i>	0.431 \pm 0.001	0.432 \pm 0.003	\uparrow 2.1%
	24/24	0.401 \pm 0.001	<i>0.411 \pm 0.001</i>	0.506 \pm 0.002	0.505 \pm 0.001	\uparrow 2.4%
	36/6	0.319 \pm 0.001	<i>0.329 \pm 0.001</i>	0.365 \pm 0.001	0.363 \pm 0.004	\uparrow 3.0%
	36/12	0.347 \pm 0.001	<i>0.357 \pm 0.001</i>	0.398 \pm 0.001	0.401 \pm 0.003	\uparrow 2.8%

Table 4: Comparison of graph variants Sparse Structure Graph (GraFITi+SSG), Complete Triplet Graph (GraFITi+CTG) and Induced Triplet Graph (GraFITi+ITG) by observing 36 hrs and forecast for next 3 time points, Evaluation metric is MSE, lower the better.

Dataset	GraFITi+SSG	GraFITi+CTG	GraFITi+ITG
MIMIC-III	0.396 \pm 0.030	0.419 \pm 0.043	0.551 \pm 0.061
MIMIC-IV	0.225 \pm 0.001	0.231 \pm 0.002	0.273 \pm 0.005
Physionet'12	0.286 \pm 0.001	0.287 \pm 0.002	0.317 \pm 0.015

ter performance of GraFITi+SSG shows that the graph constructed based on the sparsity structure of the input time series is more useful for the forecasting.

Table 5: Performance of GraFITi with varying sparsity levels using MIMIC-III dataset. The ‘IMTS’ dataset refers to the actual dataset, while ‘AsTS’ is a synthetic asynchronous time series dataset created by limiting the number of channels that can be observed at each time point to one. The ‘AsTS + x%’ dataset is a modified version of the ‘AsTS’ dataset where x% of the missing observations were retrieved. Goal is to observe 36 hours of data and then forecast the next three time steps

Model	IMTS	AsTS	AsTS+10%	AsTS+50%	AsTS+90%
GraFITi	0.396	0.931	0.845	0.547	0.413
LinODENet	0.446	0.894	0.815	0.581	0.452

7.6 Limitations

The proposed GraFITi model is a powerful tool for forecasting irregularly sampled multivariate time series with missing values. It provides more accurate forecasts compared to existing state-of-the-art models even when the datasets are extremely sparse (with sparsity upto 98% in MIMIC-IV). However, we have identified a limitation in the model when it comes to data setup. Specifically, when dealing with Asynchronous Time Series datasets, where channels are observed independently and at any given point in time, no

two channels are observed, the sparse graph gets disconnected. This disconnection hinders the flow of information and can be problematic when channels have a strong correlation towards the forecasts as model may not be able to capture these correlations. It can be observed from Table 5 where GraFITi is compared with the next best baseline model LinODENet for varying sparsity levels using MIMIC-III dataset. It can be observed that the performance of GraFITi deteriorates with increase in sparsity levels and gets worst when the series become asynchronous.

Additionally, the current representation cannot handle meta data for the series. Although, we can add these meta data points as another set of channel nodes in the graph, again the graph will be disconnected because meta data points do not have edges connecting the time nodes. One possible solution to both the challenges is by connecting all the channel nodes including meta data if exists, and perform a separate multi-head attention on them.

Therefore, in future work, we aim to extend the proposed model to handle Asynchronous Time Series datasets, where the current graph representation provides a disconnected graph. We investigate the possible challenges and develop a model that can handle Asynchronous datasets and meta data in the series. This will address the limitation of GraFITi and help to capture the correlations between channels, providing more accurate forecasts.

8 Conclusions

In this paper, we propose Graph based architectures for the forecasting of irregularly sampled time series with missing values (IMTS). In this, first we represent the time series as a hybrid graph with channels and observation times as nodes and observation measurements as edges; and re-represent the task of time series forecasting as an edge detection problem in a graph. An attention based architecture is proposed for learning the interactions between the nodes and edges in the graph. We experimented on 4 datasets including 3 real world and 1 synthetic dataset for various observation and prediction ranges. The extensive experimental evaluation demonstrates that the proposed GraFITi provides su-

rior forecasts compared to the state-of-the-art IMTS forecasting models.

References

Anonymous. 2023. Latent Linear ODEs with Neural Kalman Filtering for Irregular Time Series Forecasting. In *Submitted to The Eleventh International Conference on Learning Representations*. Under review.

Baytas, I. M.; Xiao, C.; Zhang, X.; Wang, F.; Jain, A. K.; and Zhou, J. 2017. Patient subtyping via time-aware LSTM networks. In *Proceedings of the 23rd ACM SIGKDD international conference on knowledge discovery and data mining*, 65–74.

Biloš, M.; Sommer, J.; Rangapuram, S. S.; Januschowski, T.; and Günnemann, S. 2021. Neural Flows: Efficient Alternative to Neural ODEs. *Advances in Neural Information Processing Systems*, 34: 21325–21337.

Borovykh, A.; Bohte, S.; and Oosterlee, C. W. 2017. Conditional time series forecasting with convolutional neural networks. *arXiv preprint arXiv:1703.04691*.

Brocklebank, J. C.; and Dickey, D. A. 2003. *SAS for forecasting time series*. John Wiley & Sons.

Cao, D.; Wang, Y.; Duan, J.; Zhang, C.; Zhu, X.; Huang, C.; Tong, Y.; Xu, B.; Bai, J.; Tong, J.; et al. 2020. Spectral temporal graph neural network for multivariate time-series forecasting. *Advances in neural information processing systems*, 33: 17766–17778.

Cao, W.; Wang, D.; Li, J.; Zhou, H.; Li, L.; and Li, Y. 2018. Brits: Bidirectional recurrent imputation for time series. *Advances in neural information processing systems*, 31.

Che, Z.; Purushotham, S.; Cho, K.; Sontag, D.; and Liu, Y. 2018. Recurrent neural networks for multivariate time series with missing values. *Scientific reports*, 8(1): 1–12.

Chen, R. T.; Rubanova, Y.; Bettencourt, J.; and Duvenaud, D. K. 2018. Neural ordinary differential equations. *Advances in neural information processing systems*, 31.

Chen, Y.; Segovia, I.; and Gel, Y. R. 2021. Z-GCNETs: time zigzags at graph convolutional networks for time series forecasting. In *International Conference on Machine Learning*, 1684–1694. PMLR.

De Brouwer, E.; Simm, J.; Arany, A.; and Moreau, Y. 2019. GRU-ODE-Bayes: Continuous modeling of sporadically-observed time series. *Advances in neural information processing systems*, 32.

De Gooijer, J. G.; and Hyndman, R. J. 2006. 25 years of time series forecasting. *International journal of forecasting*, 22(3): 443–473.

De Sá, H. R.; and Prudêncio, R. B. 2011. Supervised link prediction in weighted networks. In *The 2011 international joint conference on neural networks*, 2281–2288. IEEE.

Fu, C.; Zhao, M.; Fan, L.; Chen, X.; Chen, J.; Wu, Z.; Xia, Y.; and Xuan, Q. 2018. Link weight prediction using supervised learning methods and its application to yelp layered network. *IEEE Transactions on Knowledge and Data Engineering*, 30(8): 1507–1518.

Horn, M.; Moor, M.; Bock, C.; Rieck, B.; and Borgwardt, K. 2020. Set functions for time series. In *International Conference on Machine Learning*, 4353–4363. PMLR.

Hou, Y.; and Holder, L. B. 2017. Deep learning approach to link weight prediction. In *2017 International Joint Conference on Neural Networks (IJCNN)*, 1855–1862. IEEE.

Johnson, A.; Bulgarelli, L.; Pollard, T.; Horng, S.; and Celi, L. 2021. *Mark. R. MIMIC-IV (version 1.0)*. PhysioNet.

Johnson, A. E.; Pollard, T. J.; Shen, L.; Lehman, L.-w. H.; Feng, M.; Ghassemi, M.; Moody, B.; Szolovits, P.; Anthony Celi, L.; and Mark, R. G. 2016. MIMIC-III, a freely accessible critical care database. *Scientific data*, 3(1): 1–9.

Kipf, T. N.; and Welling, M. 2017. Semi-Supervised Classification with Graph Convolutional Networks. In *International Conference on Learning Representations*.

Krishnan, R.; Shalit, U.; and Sontag, D. 2017. Structured inference networks for nonlinear state space models. In *Proceedings of the AAAI Conference on Artificial Intelligence*, volume 31.

Krishnan, R. G.; Shalit, U.; and Sontag, D. 2015. Deep kalman filters. *arXiv preprint arXiv:1511.05121*.

Kumar, S.; Spezzano, F.; Subrahmanian, V.; and Faloutsos, C. 2016. Edge weight prediction in weighted signed networks. In *2016 IEEE 16th International Conference on Data Mining (ICDM)*, 221–230. IEEE.

Lee, J.; Lee, Y.; Kim, J.; Kosiorek, A.; Choi, S.; and Teh, Y. W. 2019. Set transformer: A framework for attention-based permutation-invariant neural networks. In *International conference on machine learning*, 3744–3753. PMLR.

Li, S.; Jin, X.; Xuan, Y.; Zhou, X.; Chen, W.; Wang, Y.-X.; and Yan, X. 2019. Enhancing the locality and breaking the memory bottleneck of transformer on time series forecasting. *Advances in neural information processing systems*, 32.

Li, S. C.-X.; and Marlin, B. M. 2015. Classification of Sparse and Irregularly Sampled Time Series with Mixtures of Expected Gaussian Kernels and Random Features. In *UAI*, 484–493.

Lim, B.; and Zohren, S. 2021. Time-series forecasting with deep learning: a survey. *Philosophical Transactions of the Royal Society A*, 379(2194): 20200209.

Lipton, Z. C.; Kale, D.; and Wetzel, R. 2016. Directly modeling missing data in sequences with rnns: Improved classification of clinical time series. In *Machine learning for healthcare conference*, 253–270. PMLR.

Livieris, I. E.; Pintelas, E.; and Pintelas, P. 2020. A CNN-LSTM model for gold price time-series forecasting. *Neural computing and applications*, 32: 17351–17360.

Menne, M. J.; Williams Jr, C.; and Vose, R. S. 2015. United States historical climatology network daily temperature, precipitation, and snow data. *Carbon Dioxide Information Analysis Center, Oak Ridge National Laboratory, Oak Ridge, Tennessee*.

Murata, T.; and Moriyasu, S. 2007. Link prediction of social networks based on weighted proximity measures. In *IEEE/WIC/ACM International Conference on Web Intelligence (WI'07)*, 85–88. IEEE.

Newbold, P. 1983. ARIMA model building and the time series analysis approach to forecasting. *Journal of forecasting*, 2(1): 23–35.

Oord, A. v. d.; Dieleman, S.; Zen, H.; Simonyan, K.; Vinyals, O.; Graves, A.; Kalchbrenner, N.; Senior, A.; and Kavukcuoglu, K. 2016. Wavenet: A generative model for raw audio. *arXiv preprint arXiv:1609.03499*.

Rubanova, Y.; Chen, R. T.; and Duvenaud, D. K. 2019. Latent ordinary differential equations for irregularly-sampled time series. *Advances in neural information processing systems*, 32.

Sagheer, A.; and Kotb, M. 2019. Time series forecasting of petroleum production using deep LSTM recurrent networks. *Neurocomputing*, 323: 203–213.

Satorras, V. G.; Rangapuram, S. S.; and Januschowski, T. 2022. Multivariate time series forecasting with latent graph inference. *arXiv preprint arXiv:2203.03423*.

Shukla, S. N.; and Marlin, B. 2022. Heteroscedastic Temporal Variational Autoencoder For Irregularly Sampled Time Series. In *International Conference on Learning Representations*.

Shukla, S. N.; and Marlin, B. M. 2021. Multi-time attention networks for irregularly sampled time series. *arXiv preprint arXiv:2101.10318*.

Siami-Namini, S.; Tavakoli, N.; and Namin, A. S. 2019. The performance of LSTM and BiLSTM in forecasting time series. In *2019 IEEE International Conference on Big Data (Big Data)*, 3285–3292. IEEE.

Silva, I.; Moody, G.; Scott, D. J.; Celi, L. A.; and Mark, R. G. 2012. Predicting in-hospital mortality of icu patients: The physionet/computing in cardiology challenge 2012. In *2012 Computing in Cardiology*, 245–248. IEEE.

Tashiro, Y.; Song, J.; Song, Y.; and Ermon, S. 2021. CSDI: Conditional score-based diffusion models for probabilistic time series imputation. *Advances in Neural Information Processing Systems*, 34: 24804–24816.

Vaswani, A.; Shazeer, N.; Parmar, N.; Uszkoreit, J.; Jones, L.; Gomez, A. N.; Kaiser, Ł.; and Polosukhin, I. 2017. Attention is all you need. *Advances in neural information processing systems*, 30.

Velickovic, P.; Cucurull, G.; Casanova, A.; Romero, A.; Lio, P.; and Bengio, Y. 2017. Graph attention networks. *stat*, 1050: 20.

Wu, H.; Xu, J.; Wang, J.; and Long, M. 2021. Autoformer: Decomposition transformers with auto-correlation for long-term series forecasting. *Advances in Neural Information Processing Systems*, 34: 22419–22430.

Wu, Z.; Pan, S.; Long, G.; Jiang, J.; Chang, X.; and Zhang, C. 2020. Connecting the dots: Multivariate time series forecasting with graph neural networks. In *Proceedings of the 26th ACM SIGKDD International Conference on Knowledge Discovery & Data Mining*, 753–763.

Yalavarthi, V. K.; Burchert, J.; and Schmidt-Thieme, L. 2022a. DCSF: Deep Convolutional Set Functions for Classification of Asynchronous Time Series. In *2022 IEEE 9th International Conference on Data Science and Advanced Analytics (DSAA)*, 1–10.

Yalavarthi, V. K.; Burchert, J.; and Schmidt-Thieme, L. 2022b. Tripleformer for Probabilistic Interpolation of Asynchronous Time Series. *arXiv preprint arXiv:2210.02091*.

Yang, X.; and Wang, B. 2020. Local ranking and global fusion for personalized recommendation. *Applied Soft Computing*, 96: 106636.

You, J.; Ma, X.; Ding, Y.; Kochenderfer, M. J.; and Leskovec, J. 2020. Handling missing data with graph representation learning. *Advances in Neural Information Processing Systems*, 33: 19075–19087.

Zeng, A.; Chen, M.; Zhang, L.; and Xu, Q. 2022. Are transformers effective for time series forecasting? *arXiv preprint arXiv:2205.13504*.

Zhao, J.; Miao, L.; Yang, J.; Fang, H.; Zhang, Q.-M.; Nie, M.; Holme, P.; and Zhou, T. 2015. Prediction of links and weights in networks by reliable routes. *Scientific reports*, 5(1): 12261.

Zhou, H.; Zhang, S.; Peng, J.; Zhang, S.; Li, J.; Xiong, H.; and Zhang, W. 2021. Informer: Beyond efficient transformer for long sequence time-series forecasting. In *Proceedings of the AAAI Conference on Artificial Intelligence*, volume 35, 11106–11115.

Zhou, T.; Ma, Z.; Wen, Q.; Wang, X.; Sun, L.; and Jin, R. 2022. FEDformer: Frequency Enhanced Decomposed Transformer for Long-term Series Forecasting. In *Proceedings of the 39th International Conference on Machine Learning*, volume 162 of *Proceedings of Machine Learning Research*, 27268–27286. PMLR.

Zulaika, U.; Sanchez-Corcuera, R.; Almeida, A.; and Lopez-de Ipina, D. 2022. LWP-WL: Link weight prediction based on CNNs and the Weisfeiler–Lehman algorithm. *Applied Soft Computing*, 120: 108657.

A Ablation studies

A.1 Importance of target edge

In the current graph representation target edges are connected in the graph providing rich embedding to learn the edge weight. However, we would like to see the performance of the model without query edges in the graph. For this, we compared the experimental results of GraFITi and GraFITi-T where GraFITi-T is the same architecture without query edges in the graph. The predictions are made after $L - 1^{\text{th}}$ layer by concatenating the channel embedding and the sinusoidal embedding of the query time node and passing it through the dense layer. The results for the real IMTS datasets are reported in Table 6.

Table 6: Performance of GraFITi-T (GraFITi without query edges in the graph), evaluation metric MSE.

Model	MIMIC-III	MIMIC-IV	Physionet'12
GraFITi	0.396 ± 0.030	0.225 ± 0.001	0.286 ± 0.001
GraFITi-T	0.433 ± 0.019	0.269 ± 0.001	0.288 ± 0.001

It can be seen that the performance of the GraFITi deteriorated significantly without query edges in the graph. GraFITi exploit the sparse structure in the graph for predicting the weight of the query edge. The attention mechanism help the target edge to gather the useful information from the incident nodes.

A.2 MAB vs GAT as gnn module

Table 7: Comparing performance of MAB (GraFITi-MAB) and GAT (GraFITi-GAT) as gnn module in GraFITi.

	MIMIC-III	MIMIC-IV	Physionet'12
GraFITi-MAB	0.396 ± 0.030	0.225 ± 0.001	0.286 ± 0.001
GraFITi-GAT	0.388 ± 0.020	0.225 ± 0.001	0.288 ± 0.001

In Table 7, we compare the performance of MAB and GAT as a gnn module in the proposed GraFITi using MIMIC-III, MIMIC-IV and Physionet'12. We notice that the performance of MAB and GAT are similar. Hence, we use MAB as the gnn module in the proposed GraFITi. Please note that the purpose of this research is not to fine the best gnn module but to provide graph representation to the IMTS preserving the structure of the time series.

B Hyperparameter search

We search the following hyperparameters for IMTS forecasting models as mentioned in the respective works:

GRU-ODE-Bayes: We set the number of hidden layers to 3 and selected solver from {euler, dopri}

Neural Flows We searched for the flow layers from {1, 4} and set the hidden layers to 2

LinODENet We searched for hidden size from {64, 128}, latent size from {128, 192}. We set the encoder with 5-block ResNet with 2 ReLU pre-activated layers each, StackedFilter of 3 KalmanCells, with linear one in the beginning.

GraFITi+CTG This is the application of GraFITi over Complete Triplet Graph Representation. Hyperparameter search space is same as the GraFITi.

GraFITi+ITG This is the application of GraFITi over Induced Triplet Graph Representation. Again, the hyperparameter search space is same as the GraFITi with addition to the the number of induced nodes searched from {8,16,32,64}.

For the all the MTS forecasting models, we used the default hyperparameters provided in (Zeng et al. 2022).